

# Impulse Array Antenna Design Using Particle Swarm Optimization

Wade Brinkman

National Defence, Louis St-Laurent Building, 555 Boulevard de la Carrière,  
Gatineau, Quebec KIA 0K2, Canada

and

Michael A. Morgan\*

Department of Electrical and Computer Engineering, Naval Postgraduate School,  
Monterey, California 93950

*The particle swarm optimization algorithm is applied to the design of impulse dipole array antennas utilizing passive straight-wire reflectors. The goal is to maximize the peak squared electric field strength at a specified location in the near field of the antenna for various driving voltage waveforms. The algorithm relies on a rapid computational engine for evaluation of currents and near fields that is based on numerical solution of the Hallén time-domain integral equation. Convergence of the algorithm is shown with improvements in peak squared field exceeding 100% compared to a standard near-field focus array employing elliptical reflector placement.*

**KEYWORDS:** Impulse array, Near-field focus, Particle swarm optimization

## Nomenclature

$E_{\max}^2$	peak squared electric field at $(x_0, y_0, z_0)$ , known as the fitness value
$K$	constriction factor for updating the velocities of the swarm
$(x_n, y_n, a_n, L_n)$	location, radius, and length parameters for each reflector wire
$(x_0, y_0, z_0)$	Cartesian coordinates for the near-field focus location
$v_{\max}$	maximum velocity for a parameter in the swarm coordinate space
$v_{n,k}$	velocity of the $k$ th vector parameter of the $n$ th particle in the swarm
$\rho_1, \rho_2$	attraction parameters for global best and local best locations in the swarm
$\psi_{n,k}$	value of the $k$ th vector parameter of the $n$ th particle in the swarm

## 1. Introduction

Antennas that optimally focus peak impulsive fields into localized regions are of interest for use in emerging systems that neutralize command and control networks, as well as remotely triggered explosive devices. Impulse arrays are a particularly useful class of

---

Received March 23, 2006; revision received February 4, 2007.

\*Corresponding author; e-mail: mmorgan@nps.edu.

antennas for such missions. Their design involves a complicated matching of the structure to the excitation waveform to deliver the highest peak field within the desired focal region. Although a rough design can be made using array concepts and time-of-arrival principles, precise analysis of transient interactions between the array elements is a critical requirement for optimization. An optimal design thus requires an accurate computational method coupled to an intelligent search algorithm.

Genetic algorithms (GA) have been applied for several years to optimal antenna design, typically involving pattern specification and impedance matching over a designated frequency passband.<sup>1</sup> Recently, particle swarm optimization (PSO) was proposed as an alternative to GA for use in antenna design.<sup>5</sup> Although GA and PSO approaches both emulate aspects of natural processes, they are implemented quite differently and appear to be complementary in searching the parameter space for an optimal solution.<sup>2</sup>

## 2. Computational Procedure

Hallén's time-domain integral equation (TDIE) is an accurate means of predicting the induced currents and resultant fields generated by an impulse array antenna. The original derivation of the Hallén TDIE can be found in Ref. 3. The TDIE was programmed in MatLab<sup>4</sup> to provide rapid cost function evaluations to implement the PSO algorithm. The goal is to find the optimal impulse array geometry that maximizes the peak squared electric field via its squared magnitude at a specified location,  $(x_0, y_0, z_0)$ :

$$E_{\max}^2 = \max_{\text{time}} \{ E_x^2(x_0, y_0, z_0, t) + E_y^2(x_0, y_0, z_0, t) + E_z^2(x_0, y_0, z_0, t) \}. \quad (1)$$

This value will be termed the "fitness" in the PSO algorithm.

The PSO algorithm is applied here to 5-element and 10-element impulse arrays, each being driven by two different waveforms. These arrays have a single fixed-dipole radiator and passive reflective wire elements whose lengths, positions, and radii are varied as part of the optimization procedure. Initial element layout, as described in Ref. 4, is based on a parabolic cylinder with the element lengths and radii based on the reflector element of a Yagi antenna. These "standard" array configurations, which serve as reference values for optimization improvements, are shown in Figs. 1 and 2 for the 5- and 10-element cases. Wire elements are parallel and  $z$  directed with centers at  $z = 0$  and locations specified by their  $(x, y)$  coordinates. The driven dipole is located at  $(0, 0)$ .

The two waveforms used are an exponential step and a damped sine. The exponential step, as shown in Fig. 3, initiates at 5 ns, with a 5-ns exponential rise time and a run time of 100 ns. The damped sine, shown in Fig. 4, starts at 10 ns. It has an exponential decay time constant of 100 ns and a center frequency of 20 MHz, with a run time of 500 ns. The reference point is located on boresight at 5 m from the driven element:  $(x_0, y_0, z_0) = (5, 0, 0)$  m. The transient electric and magnetic fields produced at the reference location due to the two excitation waveforms applied to the standard 5- and 10-element arrays are shown by dashed lines in Figs. 10, 11, 14, 15, 18, 19, 21, and 22. As expected, the 10-element standard array produces a larger field than the 5-element standard configuration for the same excitation.

## 3. Particle Swarm Optimization

PSO is an evolutionary search technique that was recently proposed for electromagnetic design due to its ability to optimally solve complex engineering problems with many degrees

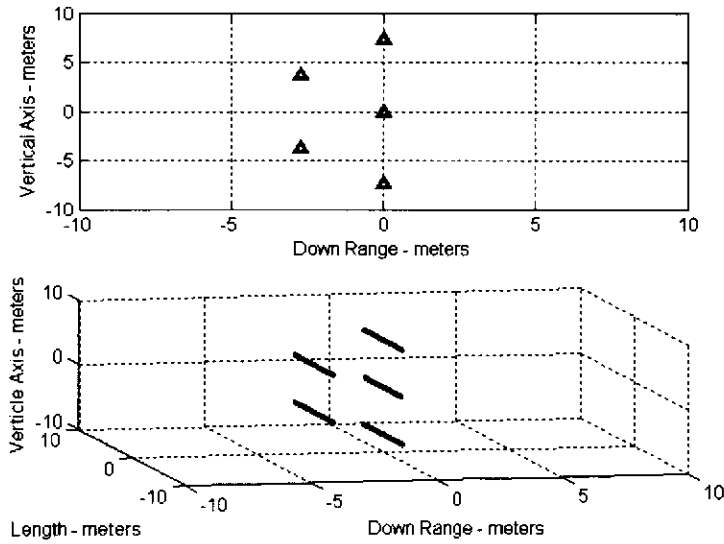


Fig. 1. Five-element impulse array.

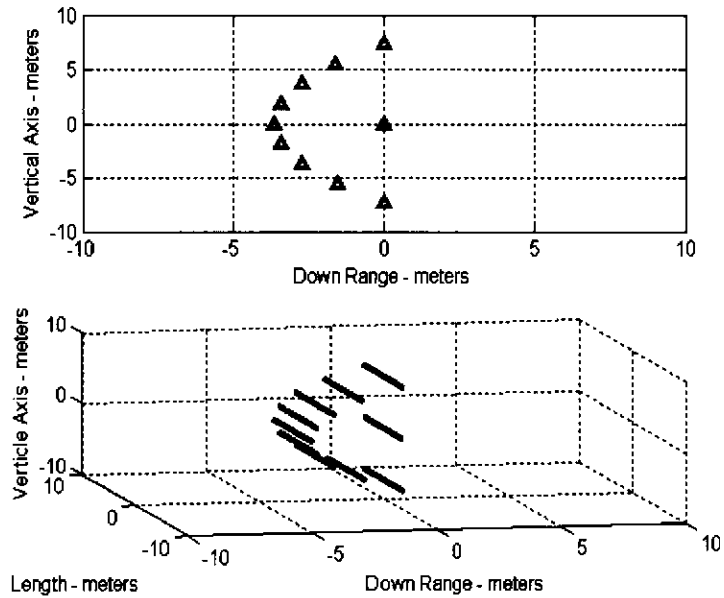


Fig. 2. Ten-element impulse array.

of freedom. PSO finds its basis in the observation that the way that fish school and bees swarm in their search for food is optimal in nature. A detailed explanation of the PSO is given by Robinson and Rahmat-Samii.<sup>5</sup> This was used as a reference to construct the optimization of the impulse array antenna. The PSO for the impulse array optimization task follows the flowchart in Fig. 5. It possesses the following basic steps:

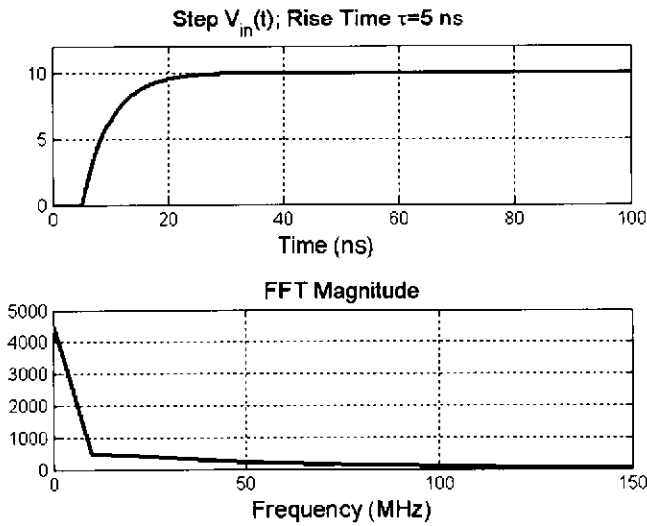


Fig. 3. Exponential step waveform.

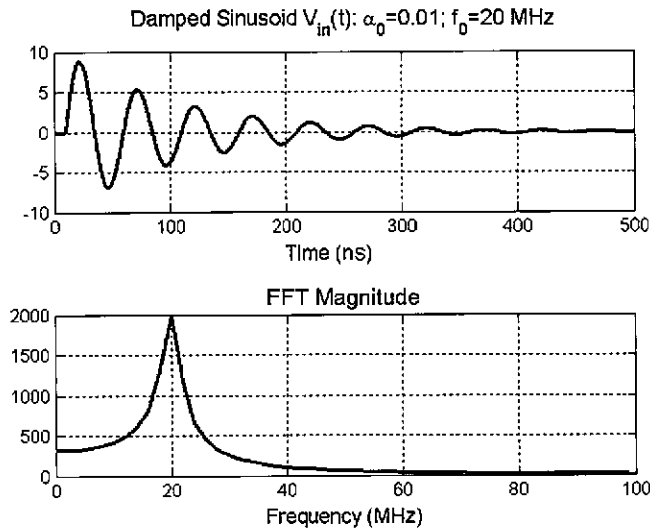


Fig. 4. Damped sine waveform.

1. Initialize the swarm.
2. Evaluate fitness of each particle in the swarm and assign local and global bests.
3. Update swarm velocities.
4. Update swarm positions.
5. Update fitness and local and global bests.
6. Check whether search is complete.

The first stage is to initialize the particles in the swarm. There are four degrees of freedom for each reflector element that affect  $E_{max}^2$  at the field point  $(x_0, y_0, z_0)$ . These are the location

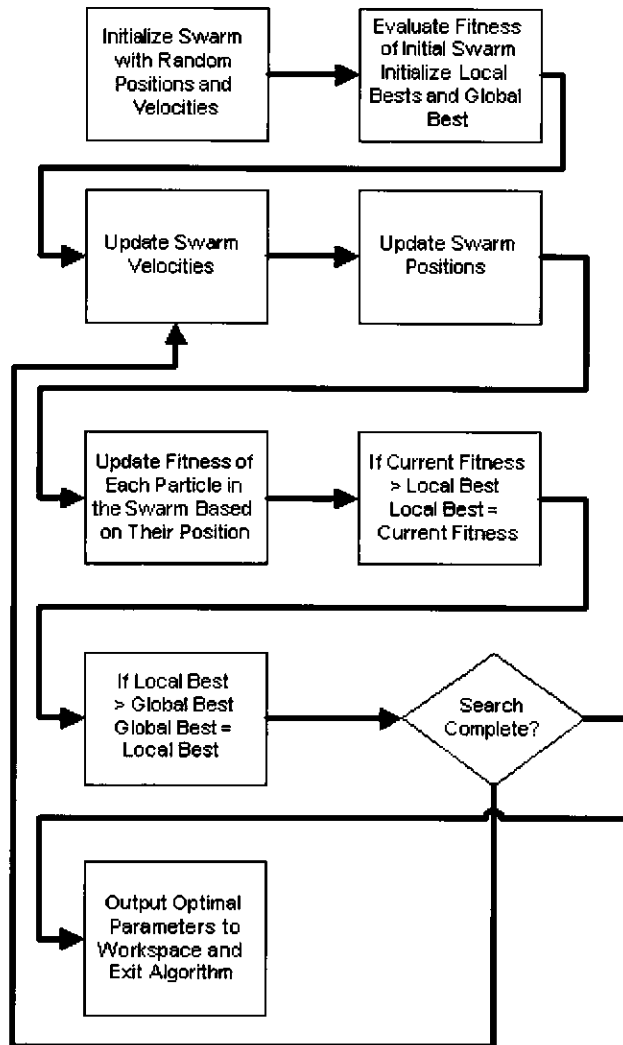


Fig. 5. PSO flowchart.<sup>5</sup>

coordinates  $x_n$  and  $y_n$ , radius  $a_n$ , and length  $L_n$ . The location of the driven element is maintained at  $(0, 0)$  while its radius and length are adjusted. In the initial application only the reflector locations were searched. However, this produced only minimal improvements. A more significant increase in  $E_{\max}^2$  is achieved when the lengths and radii are also searched for all elements.

The search space for an  $N$ -element array has dimension  $M = 4(N - 1) + 2$  due to the four degrees of freedom for each reflector and two degrees of freedom for the driven element. For the 5-element impulse array, each particle in the swarm will have a "coordinate" vector of  $M = 18$  parameters. Each particle for the 10-element impulse array has a coordinate location with  $M = 38$  parameters to search.

The next step is to decide on a reasonable range of values for each parameter, thus bounding the  $M$ -dimensional solution space. The bounds of the dimensions are set as follows:  $x_n \in (-10, 0)$ ;  $y_n \in (-10, 10)$ ;  $a_n \in (0.5 \min\{a_n\}, 1.5 \max\{a_n\})$  and  $L_n \in (0.5 \min\{L_n\}, 1.5 \max\{L_n\})$ . The min–max values that bound the radius and length of elements is determined from the parameter set used to define the standard array built using elliptically distributed locations of the reflectors with lengths and radii of a Yagi array.

Once the solution space has been defined, the swarm can be defined. Each element of each particle is assigned a value that is linearly random within its applicable range of values. For example, each vector element of each particle contained within the swarm, which represents the  $x_n$  coordinate, is assigned a value determined from

$$x_n = -10 + 10 \text{ rand}(0, 1), \quad (2)$$

where rand is a random number uniformly distributed between (0, 1). The other parameters are assigned values in a similar fashion.

The second part of swarm initialization is to assign each element of each particle a vector velocity that is linearly random between  $\pm v_{\max}$ . Robinson and Rahmat-Samii<sup>5</sup> state that an optimal  $v_{\max}$  is equal to the expanse of the solution space in the applicable dimension. For example, a vector element representing the  $x_n$  dimension in a particle would have  $v_{\max} = 10$ .

Figures 6 and 7 illustrate the initial layout of the swarm for each of the degrees of freedom. As expected, the elements are evenly dispersed between their boundary conditions. The efficiency of the PSO and the completeness of the search depend on the particles being scattered randomly throughout the solution space.

Since the solution space is extensive, a known optimal solution, such as the standard design in Fig. 1, is inserted into the swarm. This allows for a bias toward this known optimal solution and gives the PSO a good starting point since, as will shortly be shown, the global best particle affects the search pattern of the entire swarm. Also, with the remainder

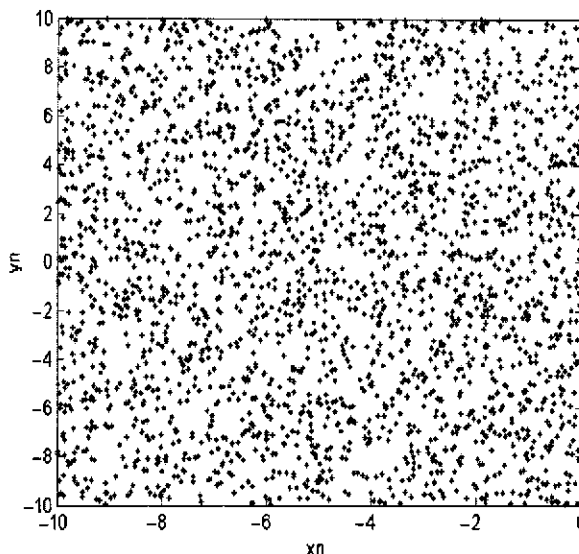


**Fig. 6.** Plot of the  $x_n$  vs.  $y_n$  in the initial 500-particle swarm.

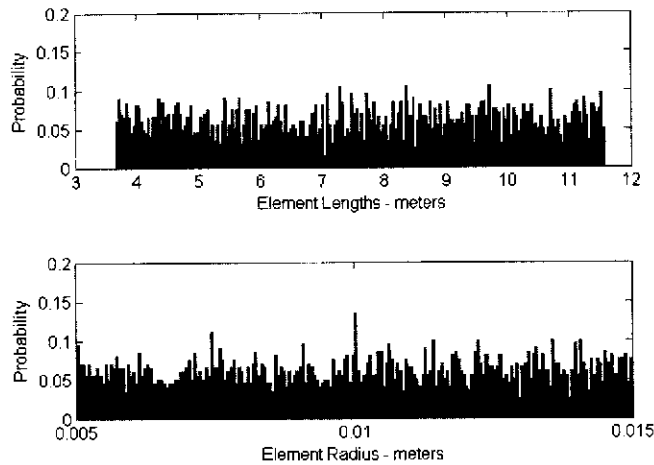


**Fig. 7.** Histogram of the distribution of  $a_n$  and  $L_n$  in the initial swarm.

of the swarm randomly initialized, the PSO algorithm still performs a complete search of the solution space despite this bias.

Evaluation of the fitness of each particle is essential to any evolutionary search, and the PSO is no exception. The result of the fitness calculation is crucial in forming the search pattern of the solution space. At this point, Hallén's TDIE is applied to all particles in the swarm to produce a value for  $L_{\max}^2$  evaluated at the test point 5 m on boresight  $(x_0, y_0, z_0) = (5, 0, 0)$  m. The goal is to find an impulse antenna array layout that gives  $\max\{L_{\max}^2\}$ .

At this point, it is important to discuss two factors that affect the calculation of the fitness. The first is collision of elements in the solution space. Because the PSO can consider any configuration in searching for a maximum to Eq. (1), there is a possibility that the antenna elements in a given solution may end up at the same location coordinates. Not only is this an unrealistic solution, but it causes a singularity in the code. This necessitates the verification of separation of antenna elements prior to calculation of particle fitness. A minimum separation was set at 20 cm, which is 20 times greater than the 1-cm element radius of the antenna layout in Figs. 1 and 2. When particles are found to possess antenna elements in violation of the minimum distance,  $E_{\max}^2$  is set equal to zero and the cost function is not called.

The second issue is the setting of the time interval and the number of time increments in the calculation. The time interval is essential because it must be suitably long in order to give the waveform time to build up to a maximum but not so long that the run time is excessive. The number of time increments determines the number of nodes on each antenna element and is essential to the accuracy of the calculation. However, increased accuracy equates to a significantly longer run time. Also, care must be taken to avoid setting the number of time increments too low, especially when using the damped sinusoid waveform. This is because the MatLab code requires that the number of nodes be an odd integer, and with the node size increasing with a decrease in the number of time increments, rounding of the actual element lengths occurs. The exponential step waveform does not appear to be overly affected by the rounding. However, the damped sinusoid requires a much higher number of time increments to produce consistent results due to its critical requirement for

antenna element resonance. One effective way to deal with the requirement for a high time increment requirement is to run a search with a low number of time increments and find a crude optimized solution. Then run a search with a higher time increment value with the crude optimal solution inserted into the initialization of the swarm.

After each calculation of fitness, the PSO builds a vector, called GBest for global best, that contains the antenna layout that is the best ever encountered by any member of the swarm. Second, it builds a matrix containing the best antenna layout ever encountered by each particle of the swarm, which is commonly referred to as LBest, for local best. Since this is the first evaluation of fitness, each particle's current position by default forms the LBest matrix.

To update the velocity of the particles, the procedure in Ref. 5 is used:

$$v_{n,k}(p+1) = K \{v_{n,k}(p) + \rho_1 \text{rand} [\text{LBest}_{n,k} - \psi_{n,k}(p)] + \rho_2 \text{rand} [\text{GBest}_{n,k} - \psi_{n,k}(p)]\}, \quad (3)$$

where  $\psi_{n,k}(p)$  represents the value of the  $k$ th vector element of the  $n$ th particle in the swarm at the  $p$ th iteration,  $v_{n,k}(p)$  is the  $p$ th iteration velocity of the same particle and vector element, GBest is the value of the  $k$ th vector element in the global best vector, and LBest is the value of the  $k$ th vector element in that particle's local best vector.  $K$  is the constriction factor, which, as stated in Ref. 5, was optimally determined to be 0.729.  $K$  can be described as a damping effect that assists in reducing the velocity over time as LBest converges toward GBest and the search becomes more localized. The parameters  $\rho_1$  and  $\rho_2$  are equal to 2.8 and 1.3, respectively, and describe the attraction between the particle and its LBest and the swarm's GBest. When updating the velocity, it is important to ensure that no particle's velocity exceeds the  $v_{\text{max}}$  in any of its dimensions. If this occurs, this velocity is simply set equal to  $v_{\text{max}}$  for that dimension with its direction preserved.

To update the particle's position, the velocity vector of each particle is added to the current position, since the time increment is normalized to unity. What must now be verified is that no particle has exited the solution space in any one of the dimensions. Robinson and Rahmat-Samii<sup>5</sup> list three ways to deal with boundary conditions. For this research, the rebounding wall method was chosen. The rebounding wall method sets the position of a particle equal to the boundary in the dimension it has exited the solution space. It also assigns that dimension a velocity equal to  $0.1 \text{rand}(0, 1)v_{\text{max}}$  with a direction away from the boundary.

Now that each particle has a new position, they are again evaluated for fitness in the same manner as described above. Once the fitness has been evaluated, the results are compared against the results obtained by the GBest. If any particle is superior to the GBest, the GBest vector takes on this value. If not, the GBest vector stays the same. Similarly, each particle is compared to its LBest vector. If the fitness of its current position exceeds that of its LBest, then the current position becomes the particle's LBest vector.

There are several different ways to terminate a PSO search. The easiest is to give it a set number of cycles and let it run through this prescribed number. This way is preferred because there is no critical requirement for speed in this application. However, the workspace is saved after each cycle, so the progress of the PSO can be examined and exited if the search stagnates.

An example of a converged swarm (its  $x_n$  and  $y_n$  portion) is shown in Fig. 8. The GBest is superimposed on top of the swarm as triangles.



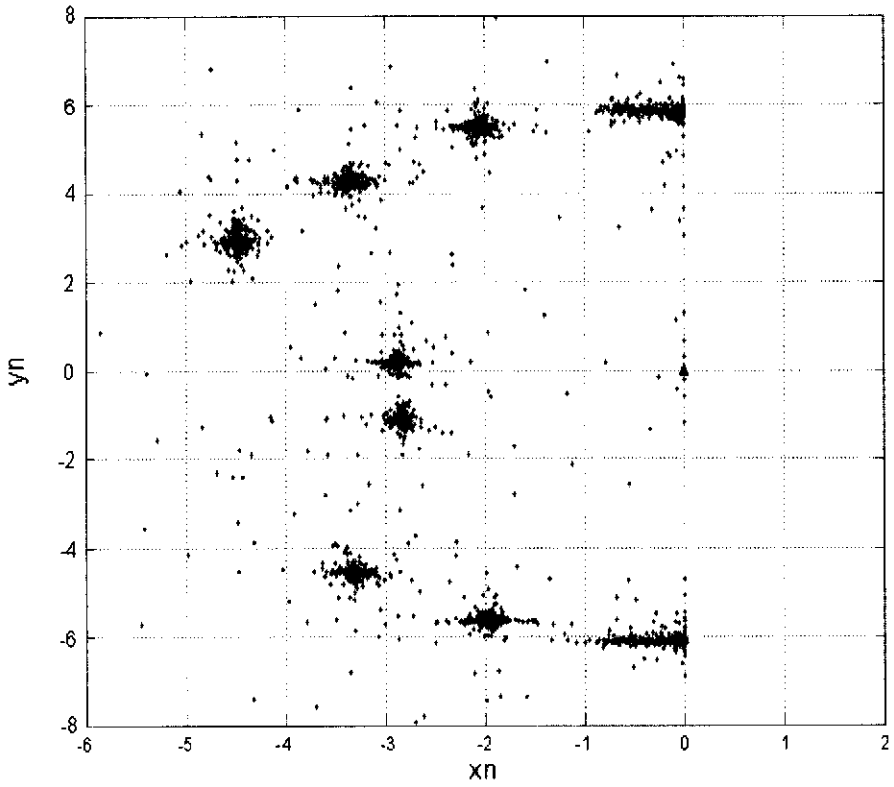


**Fig. 8.** Converged particle swarm at the end of a search.

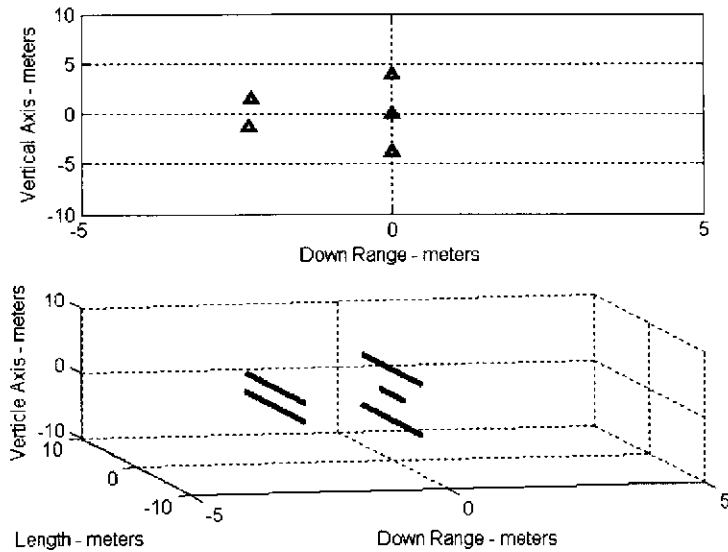


**Fig. 9.** Optimal 5-element impulse array for the exponential step waveform.

### 4. Example Computations

The optimal results were obtained by first running a coarse optimization with a lower number of time increments to ensure that the PSO would quickly calculate the swarm's fitness and pass quickly through many cycles. This optimal result was then inserted into another search that had a greater number of time increments and therefore was more accurate.

Optimizing the 5-element impulse array for the exponential step waveform, as seen in Fig. 3, results in the configuration shown in Fig. 9. Resultant E- and H-field waveforms are shown in Figs. 10 and 11. The  $\max\{E_{\max}^2\} = 0.041$ , which is an increase of 60.5% over the

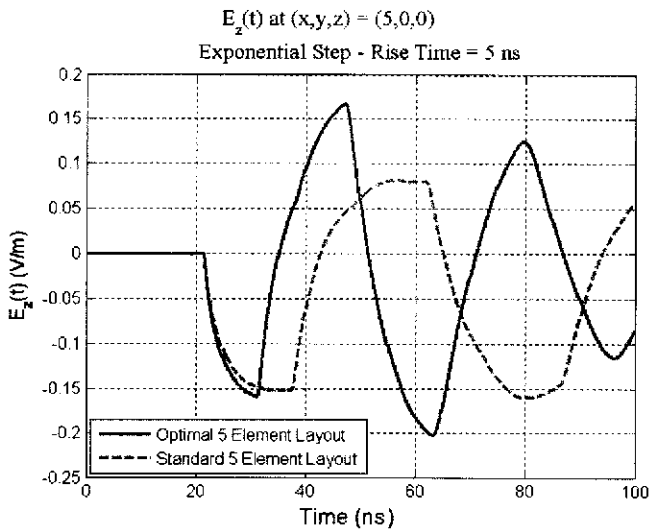


Fig. 10. Comparing E-fields for standard (Fig. 1) and optimal (Fig. 9) 5-element arrays with the exponential step waveform.

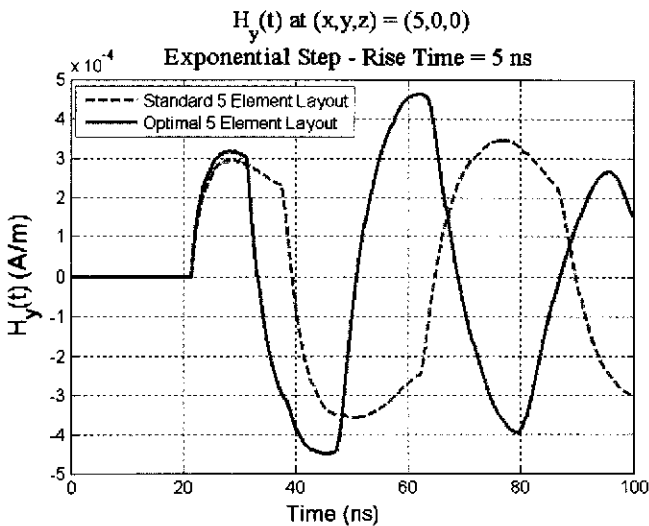
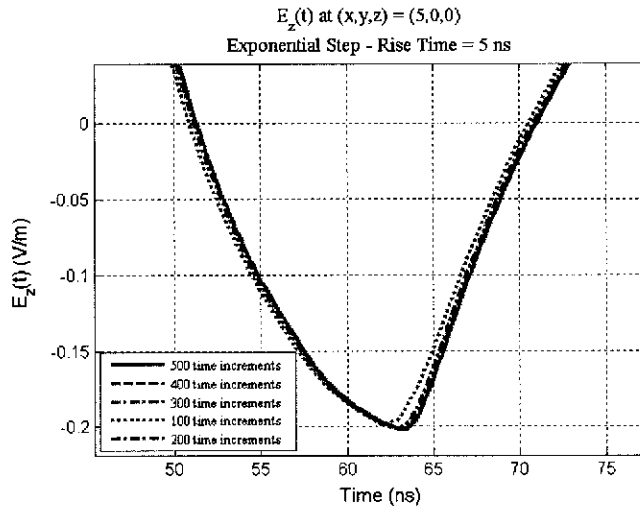


Fig. 11. Comparing H-fields for standard (Fig. 1) and optimal (Fig. 9) 5-element arrays with the exponential step waveform.

result obtained for the standard 5-element impulse array as shown in Fig. 1. It even exceeds the  $\max\{E_{\max}^2\}$  generated by the standard 10-element impulse array layout by 30%. The H-field waveform also increases the magnitude squared by 67% over that of the standard 5-element array.

It is important to prove the consistency of the results by running the simulation with different time increments. As seen in Fig. 12, changing the number of time increments does not have a significant effect on the results for time increments above 100. Even



**Fig. 12.** Waveform peak for optimal 5-element array with different time increments when driven by the exponential step waveform.

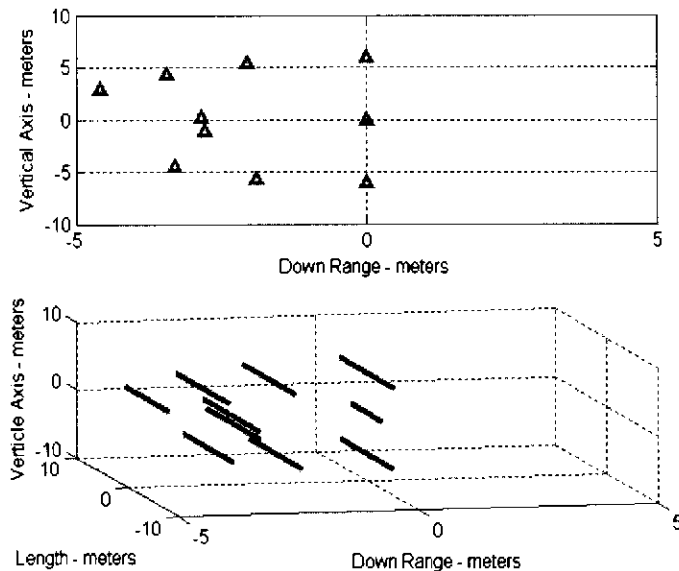


**Fig. 13.** Optimal 10-element impulse array for the exponential step waveform.

the waveform generated with 100 time increments is fairly close to the more precise answers.

Next the 10-element impulse antenna array was optimized for the exponential step waveform. The resulting layout is shown in Fig. 13, with computed E- and H-field waveforms in Figs. 14 and 15. The  $\max\{E_{\max}^2\} = 0.062$ , which is an increase of 96.5% over the result obtained for the standard 5-element impulse array as shown in Fig. 2. The H-field waveform is increased in magnitude squared by 83%.

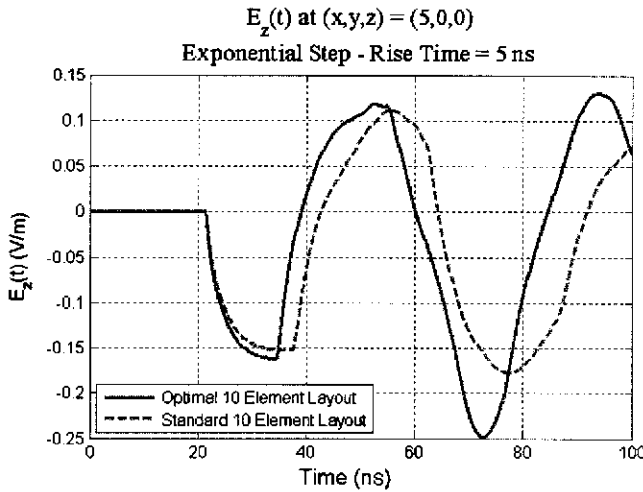


**Fig. 14.** Comparing E-fields for standard (Fig. 2) and optimal (Fig. 13) 10-element arrays with the exponential step waveform.

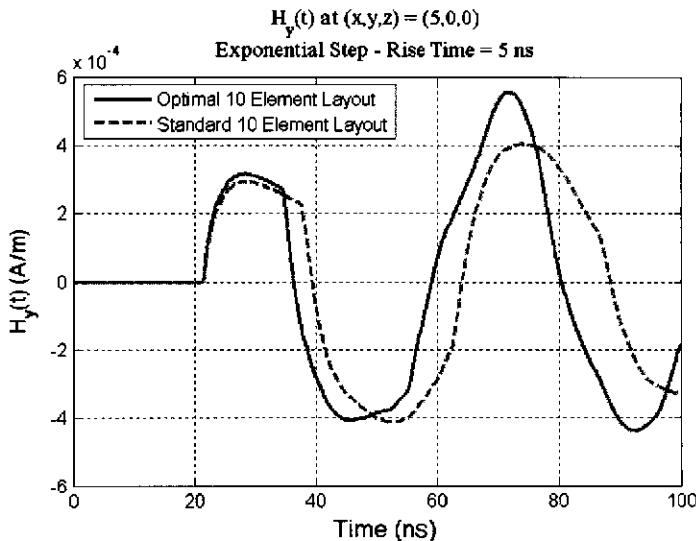


**Fig. 15.** Comparing H-fields for standard (Fig. 2) and optimal (Fig. 13) 10-element arrays with the exponential step waveform.

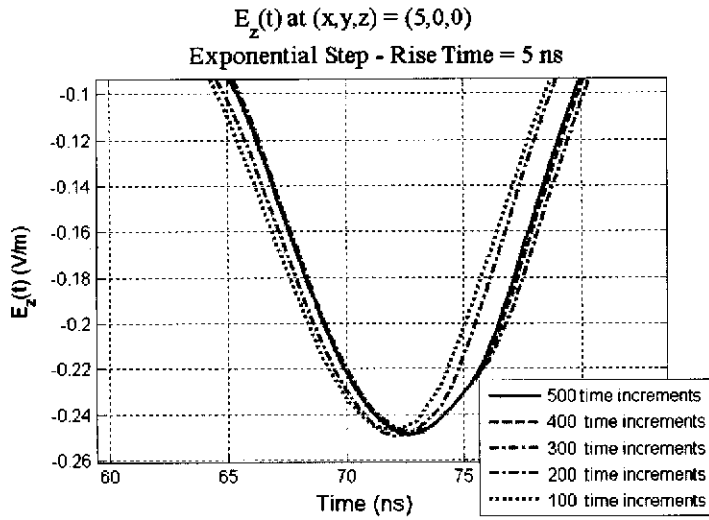


**Fig. 16.** Waveform peak for optimal 10-element array with different time increments when driven by the exponential step waveform.

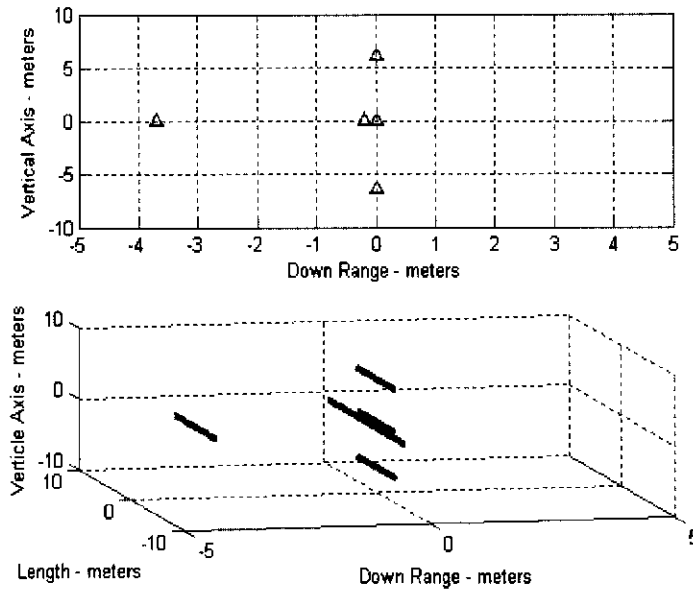


**Fig. 17.** Optimal 5-element impulse array for the damped sine waveform.

Again, we can demonstrate the consistency of the results by running the simulation with different time increments. As seen in Fig. 16, changing the number of time increments does not have a significant effect on the peak of the waveform, especially when it is set equal to or greater than 300 time increments.

Optimizing the damped sine waveform, as seen in Fig. 4, results in a 5-element impulse array as shown in Fig. 17. E- and H-field waveforms are shown in Figs. 18 and 19. The

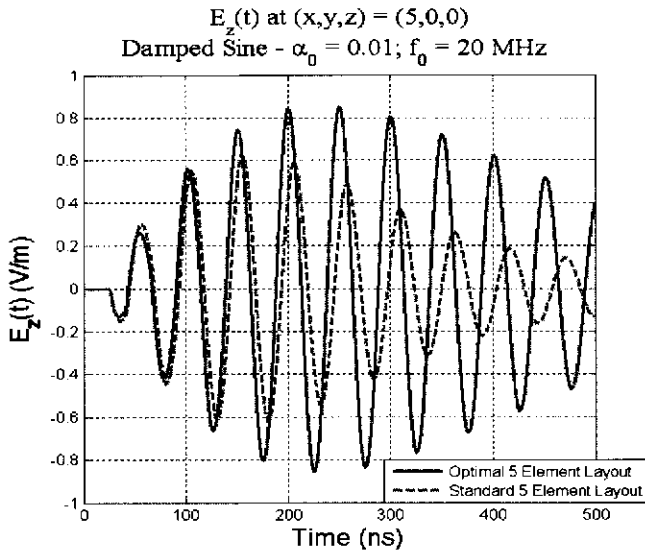


**Fig. 18.** Comparing E-fields for standard (Fig. 1) and optimal (Fig. 17) 5-element arrays with the damped sine waveform.

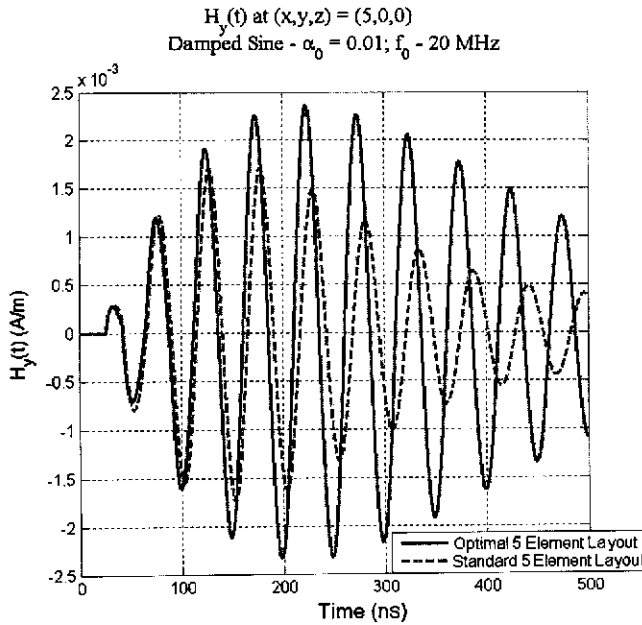


**Fig. 19.** Comparing H-fields for standard (Fig. 1) and optimal (Fig. 17) 5-element arrays with the damped sine waveform.

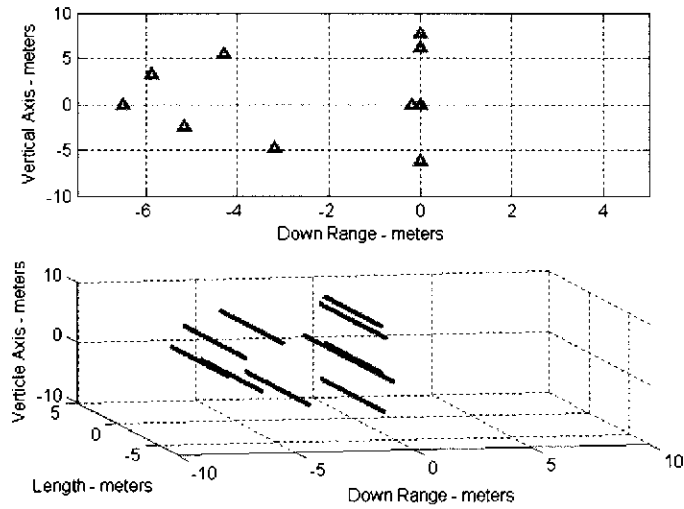


Fig. 20. Optimal 10-element impulse array for the damped sine waveform.

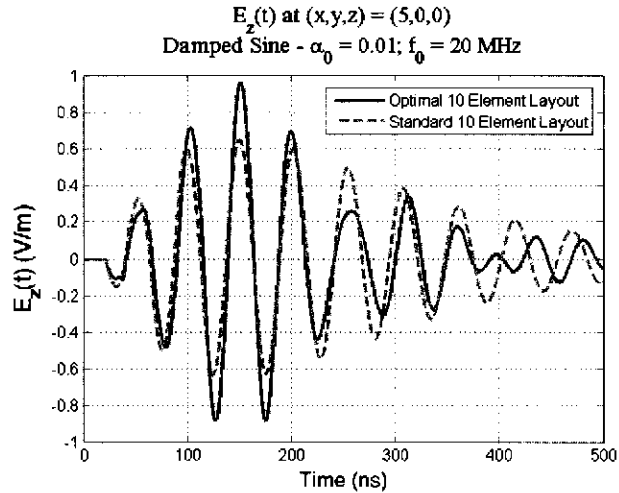
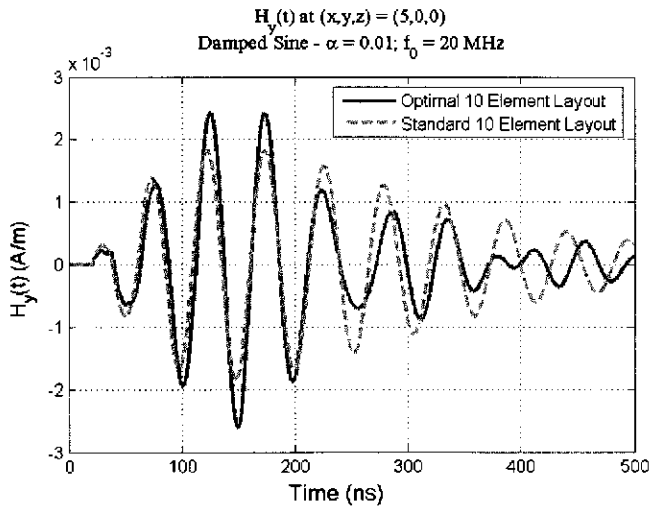


Fig. 21. Comparing E-fields for standard (Fig. 2) and optimal (Fig. 20) 10-element arrays with the damped sine waveform.

$\max\{E_{\max}^2\} = 0.7362$ , which is an increase of 85% over the result obtained for the standard 5-element impulse array. The H-field waveform is increased in magnitude squared by 83%.

The 10-element impulse antenna array was optimized for the damped sine waveform with the layout shown in Fig. 20. The E-field waveform, as shown in Fig. 21, has  $\max\{E_{\max}^2\} = 0.921$ , which is a 114% increase over the results of the standard 10-element array. Figure 22 shows the H-field waveform, which increased in magnitude squared by 113%.



**Fig. 22.** Comparing H-fields for standard (Fig. 2) and optimal (Fig. 20) 10-element array with the damped sine waveform.

## 5. Conclusions

The PSO algorithm has been applied to the design of a special class of impulse antennas to maximize the peak transient squared electric field produced at a specified near-field location. These parasitic arrays are formed from parallel wires that have a single element driven by a specified voltage waveform and several passive wire reflectors. Design parameters are the lengths, radii, and two-dimensional planar locations of the wire reflectors. Two different driving waveforms were considered, with distinct optimal array designs for each. A fast time-domain integral equation computational engine was used for evaluating performance during the optimization. Improvements were observed in peak square field exceeding 100% compared to a standard near-field focus array employing elliptical element placement.

## References

- <sup>1</sup>Altshuler, E.E., and D.S. Linden, *IEEE Trans. Antennas Propag.* **54**, 3147 (2004).
- <sup>2</sup>Boeringer, D.W., and D.H. Werner, *IEEE Trans. Antennas Propag.* **54**, 771 (2004).
- <sup>3</sup>Lui, T.K., and K.K. Mei, *Radio Sci.* **8**, 797 (1973).
- <sup>4</sup>Morgan, M.A., "Computation of Impulse Array Fields Using Hallén's Time-Domain Integral Equation," *IEEE Antennas and Propagation Society Symposium*, Monterey, CA, June 2004.
- <sup>5</sup>Robinson, J., and Y. Rahmat-Samii, *IEEE Trans. Antennas Propag.* **54**, 397 (2004).

## The Authors

**Capt. Wade Brinkman** graduated from the Royal Military College of Canada in 1997 with a Bachelors of Electrical Engineering. In 2005, he graduated from the Naval Postgraduate School in Monterey, California, with a Master of Science in Electrical Engineering (with Distinction). He currently works in Ottawa at the Canadian National Defence Headquarters, where he is the Deputy Project Manager of the Weapon Locating Sensor



project. His research interests include active electronically scanned array radars and their application to the location of rockets, artillery, and mortars.

**Dr. Michael A. Morgan** received his Ph.D. in EECS from U.C. Berkeley in 1976. He held positions at SRI International and the University of Mississippi before joining the Naval Postgraduate School (NPS) in 1979. In 1985–1986, he managed the ONR Basic Research Electromagnetics Program. Since returning to NPS, he chaired the ECE Department (1990–1995) and the Mathematics Department (1999–2002). He has contributed original research in the areas of transient scattering measurements, natural resonance target identification, finite element methods, and the design of ultrawideband impulse antennas. Professor Morgan is an IEEE Fellow and a member of URST Commission B.